Atmospheric
Chemistry
and Physics

Reactive uptake of N_2O_5 to internally mixed inorganic and organic particles: the role of organic carbon oxidation state and inferred organic phase separations

C. J. Gaston[1], J. A. Thornton[1], and N. L. Ng[2,3]

[1]Department of Atmospheric Sciences, University of Washington, Seattle, WA 98195, USA
[2]School of Chemical and Biomolecular Engineering, Georgia Institute of Technology, Atlanta, GA 30332, USA
[3]School of Earth and Atmospheric Sciences, Georgia Institute of Technology, Atlanta, GA 30332, USA

Correspondence to: J. A. Thornton (thornton@atmos.uw.edu)

Abstract. We measured N_2O_5 reactive uptake onto mixed organic/inorganic submicron particles using organic compounds with a variety of oxidation states (using mainly atomic O : C ratios as a proxy) and molecular weights. The organic mass fraction, organic molecular composition, and relative humidity (RH) were varied to assess their effects separately on the N_2O_5 uptake coefficient, $\gamma(N_2O_5)$. At a constant RH, mixtures of organic components having an O : C < 0.5 with ammonium bisulfate significantly suppressed the uptake of N_2O_5(g) compared to pure ammonium bisulfate, even at small organic mass fractions (e.g., ≤ 15 %). The effect of the organic component became less pronounced at higher RH. In general, highly oxygenated organic components (O : C > 0.8) had a smaller or even negligible impact on N_2O_5(g) uptake at all RHs probed; however, a few exceptions were observed. Notably, $\gamma(N_2O_5)$ for mixtures of ammonium bisulfate with polyethylene glycol (PEG), PEG-300 (O : C = 0.56), decreased nearly linearly as the PEG mass fraction increased at constant RH until leveling off at the value measured for pure PEG. The response of $\gamma(N_2O_5)$ to increasing PEG mass fraction was similar to that measured on ambient atmospheric particles as a function of organic mass fraction. The effects of the organic mass fraction on $\gamma(N_2O_5)$, for mixtures having an O : C < ∼ 0.8, were best described using a standard resistor model of reactive uptake assuming the particles had an RH-dependent inorganic core–organic shell morphology. This model suggests that the N_2O_5 diffusivity and/or solubility in the organic layer is up to a factor of 20 lower compared to aqueous solution particles, and

that the diffusivity, solubility, and reactivity of N_2O_5 within organic coatings and particles depend upon both RH and the molecular composition of the organic medium. We use these dependencies and ambient measurements of organic aerosol from the global aerosol mass spectrometry (AMS) database to show that the typical impact of organic aerosol components is to both uniformly decrease $\gamma(N_2O_5)$, by up to an order of magnitude depending on the RH, organic mass fraction, and O : C ratio, and to induce a stronger dependence of $\gamma(N_2O_5)$ upon RH compared to purely inorganic aqueous solutions.

1 Introduction

Heterogeneous reactions between gases and atmospheric particles play an important role in air quality and global climate (Abbatt et al., 2012; Chang et al., 2011; Liao and Seinfeld, 2005; Poschl, 2005; Solomon, 1999). The reactive uptake of N_2O_5, a major nighttime NO_x ($\equiv NO + NO_2$) reservoir species, onto particles is one such reaction that is known to be potentially important on regional and global scales (Dentener and Crutzen, 1993), but remains poorly described in atmospheric models, in part due to a lack of detailed understanding of the reaction rate and mechanism in atmospheric particles. The reactive uptake of N_2O_5 to aerosol particles is a terminal sink of NO_x and source of photolabile Cl atoms (Finlayson-Pitts et al., 1989), and thus impacts ozone formation and the lifetime of greenhouse gases such as methane

(Alexander et al., 2009; Dentener and Crutzen, 1993; Osthoff et al., 2008; Shindell et al., 2009; Thornton et al., 2010). Laboratory measurements have probed the reactive uptake coefficient, $\gamma(N_2O_5)$, defined as the probability that a colliding gas molecule (N_2O_5 in this case) will react with a particle. Measurements focused on purely inorganic aerosols tend to find relatively high values of $\gamma(N_2O_5)$ ranging from 0.015 to 0.2 so long as the particles are deliquesced (Hallquist et al., 2003; Hu and Abbatt, 1997; Kane et al., 2001; Mentel et al., 1999; Mozurkewich and Calvert, 1988; Thornton and Abbatt, 2005). However, measurements of ambient aerosols have consistently shown the presence of internally mixed inorganic and organic components (Murphy et al., 2006; Zhang et al., 2007), highlighting the need to assess N_2O_5 reactivity on these mixtures.

Studies probing the effect of pure organic aerosol as well as inorganic particle seeds coated with organics have shown that even a monolayer coating can suppress the heterogeneous uptake of N_2O_5. However, the magnitude of this surface effect is highly dependent on molecular structure and likely not broadly relevant for the majority of submicron atmospheric particles, which tend to have large organic mass fractions (χ_{OA}) (Badger et al., 2006; Cosman and Bertram, 2008; Folkers et al., 2003; McNeill et al., 2006; Riemer et al., 2009; Thornton and Abbatt, 2005; Thornton et al., 2003). Chamber-derived secondary organic aerosol (SOA) coatings on sulfate seed particles produced from the ozonolysis of α-pinene, with minimal photochemical aging, showed strong suppression of $\gamma(N_2O_5)$ even with small mass loadings of biogenic SOA (Anttila et al., 2006; Escorcia et al., 2010; Folkers et al., 2003). In spite of these studies, laboratory measurements of $\gamma(N_2O_5)$ have not been able to match ambient observations, even when organic aerosol is taken into account (Abbatt et al., 2012; Bertram et al., 2009; Brown et al., 2009; Riedel et al., 2012). As suggested in a recent modeling study by Riemer et al. (2009), these discrepancies are likely due to the formation of organic coatings that can affect $\gamma(N_2O_5)$; however, the magnitude of this effect will likely depend on organic aerosol composition, particle phase, and/or morphology. As such, a systematic study of the effect of organic molecular composition on N_2O_5 uptake, though necessary, has been lacking.

In the absence of halides, hydrolysis is expected to be the dominant driver of N_2O_5 reactive uptake, and the rate of N_2O_5 reactive uptake even on halide salt particles depends on whether the particle is crystalline or deliquesced (Finlayson-Pitts et al., 1989; Griffiths et al., 2009; Thornton and Abbatt, 2005; Thornton et al., 2003). As such, properties of organic compounds thought to affect particle water content and thus $\gamma(N_2O_5)$ include the polarity and molecular weight (Griffiths et al., 2009; Jimenez et al., 2009; Thornton et al., 2003). These properties are also thought to determine particle phase and morphology as some organics when mixed with inorganic compounds can undergo RH-dependent liquid–liquid phase separations due to a "salting-out" effect wherein the

lower polarity organic components partition into an organic coating (Bertram et al., 2011; Ciobanu et al., 2009; Erdakos and Pankow, 2004; Marcolli and Krieger, 2006; Song et al., 2012; You et al., 2012, 2013). At < 70 % RH, humidity-induced liquid–liquid phase separations are predicted to occur for particles containing organics with a low oxidation state (e.g., low O : C) (Bertram et al., 2011; You et al., 2013). Additionally, certain organics facilitate the formation of amorphous phases comprised of liquid, semi-solid, and solid (glassy) states (Koop et al., 2011; Renbaum-Wolff et al., 2013; Saukko et al., 2012; Virtanen et al., 2010; Zobrist et al., 2008). The average carbon oxidation state, which scales with the O : C ratio, and molecular weight of organic components are proposed to be predictors for these phase transitions (Bertram et al., 2011; Saukko et al., 2012).

Here we present measurements of $\gamma(N_2O_5)$ on laboratory-generated particles that are mixtures of organics with ammonium bisulfate. The organic compounds, used in mixtures or as single components, spanned a range in molecular weights, water solubility, and O : C ratios, which we use as a proxy for the average carbon oxidation state and thus organic aerosol age (Kroll et al., 2011). We show the response of $\gamma(N_2O_5)$ to variations in the mass fraction, the chemical composition of different organics, and relative humidity (RH). We discuss the results in terms of (i) which properties of the particles' organic composition are most important for accurately predicting $\gamma(N_2O_5)$; (ii) the role of phase separations and morphology; and (iii) the extent to which these laboratory measurements on synthetic mixed organic/inorganic particles are comparable to ambient measurements.

2 Methods

Measurements of $\gamma(N_2O_5)$ were made using an entrained aerosol flow tube coupled to a chemical ionization mass spectrometer (CIMS) and a combination of experimental approaches similar to those described previously (Bertram and Thornton, 2009; McNeill et al., 2006; Thornton et al., 2003). Both standard decays of N_2O_5 as a function of interaction time by moving the position of the injector containing N_2O_5 (Thornton et al., 2003) and modulation of particle concentration at constant interaction time by turning the aerosol flow on and off (Bertram and Thornton, 2009) were used in this experiment. Mixed organic/inorganic aerosol were generated using a constant output atomizer using dilute solutions similar to the approach of McNeill et al. (2006). Figure 1 shows the experimental set-up used for this work.

2.1 Aerosol generation and characterization

The solutions used in this manuscript are summarized in Table 1 along with the corresponding χ_{OA} (in the aerosol) and $\gamma(N_2O_5)$ values. Three types of aqueous solutions were used to generate aerosol: (1) single component solutions (e.g.,
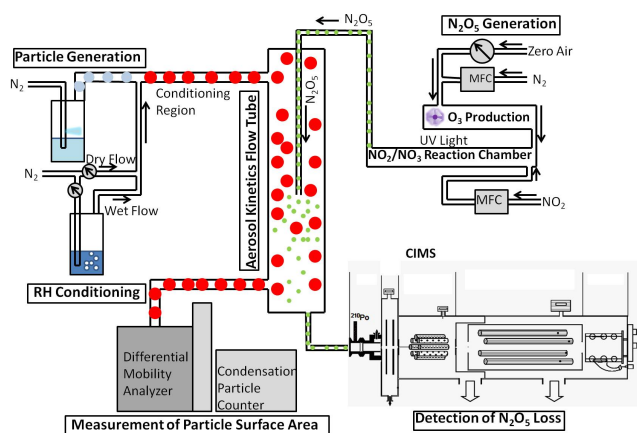
Figure 1. Schematic of the laboratory set-up used to measure $\gamma(N_2O_5)$ on laboratory-generated aerosols. A movable injector is used to change the amount of exposure time between N_2O_5 (represented by small green dots) and the generated particles (large red dots). The N_2O_5 decay is monitored using a chemical ionization mass spectrometer (CIMS) while total particle surface area (S_a) is monitored using a scanning mobility particle sizer (SMPS).

ammonium bisulfate or polyethylene glycol, PEG); (2) solutions of ammonium bisulfate and a single organic component (e.g., ammonium bisulfate/azelaic acid); and (3) ammonium bisulfate solutions containing a mix of organic components with either a high average O : C atomic ratio of 1.13 or a low average O : C atomic ratio of 0.48. Ammonium bisulfate was chosen as the inorganic component because it does not crystallize at RHs used in this work (e.g., 30–70 % RH), ensuring a deliquesced inorganic solution (Martin, 2000; Tang and Munkelwitz, 1977, 1994). Ammonium bisulfate (Alfa Aesar, 99.9 % purity), azelaic acid (Acros Organics, 98 % purity), (1,2,9)-nonanetriol (Sigma, purity unknown), polyethylene glycol with an average molecular weight of 300 g mol^{-1} (chemical formula H(OCH$_2$CH$_2$)$_n$OH) (Aldrich), citric acid, (2,5)-dihydroxy benzoic acid (gentisic acid), D-(+)-glucose, malonic acid, and succinic acid (all Sigma-Aldrich with a purity of 98 % or higher) were used as the aerosol components. Citric acid, glucose, malonic acid, and succinic acid were used to create the high O : C mixture, while azelaic acid, gentisic acid, 1,2,9-nonanetriol, and PEG were used to generate the low O : C mixture, as denoted in Table 1.

Particles were generated using a constant output atomizer (TSI Inc., Model 3076). The atomizer output was diluted and conditioned for approximately 1 min by mixing 3.3 to 4 standard liters per minute (slpm) of humidified ultra-high purity (UHP) N_2 with the atomizer output. The humidity of the dilution flow was adjusted so that the aerosol flow was at the desired RH determined with a Vaisala humidity probe (accuracy ±2 %) just upstream of the flow reactor.

Approximately 2.3–3 slpm of the conditioned aerosol flow was continuously drawn through the flow reactor via a side arm at the top of the flow tube by means of a critical orifice

on the CIMS inlet. Particle size distributions and total surface area concentrations (S_a) at the flow tube exit were measured using a scanning mobility particle sizer (SMPS) consisting of a differential mobility analyzer and condensation particle counter (TSI Inc. or Grimm Technologies; both instruments gave similar distributions). S_a typically ranged from 0.8 to 7.0×10^{-4} cm^2 cm^{-3}. Example surface area-weighted size distributions resulting from atomizing an ammonium bisulfate solution containing various amounts of PEG (i.e., mixture type 2 above) are shown in Fig. 2. The single mode, and a mean diameter that increases monotonically with increasing PEG content at constant ammonium bisulfate, suggest particles are internal mixtures of PEG and ammonium bisulfate. To ensure the measured S_a was representative of the flow tube conditions, the DMA sheath flow was conditioned to the appropriate RH by sampling from the flow reactor for ∼ 1 h prior to the start of the experiment.

2.2 N_2O_5 generation and detection

The method used to generate N_2O_5 has been discussed previously (Bertram and Thornton, 2009; Bertram et al., 2009; Lopez-Hilfiker et al., 2012; Riedel et al., 2012). As shown in Fig. 1, NO_3 is generated by reaction of NO_2 and O_3. NO_3 is then allowed to react further with excess NO_2 to produce N_2O_5 in equilibrium with NO_2 and NO_3 at room temperature (298 K). The N_2O_5 is introduced axially down the center of the flow reactor in a 0.1 slpm UHP N_2 carrier flow through a Teflon-lined movable stainless steel injector (Bertram and Thornton, 2009). N_2O_5 was detected using iodide adduct CIMS (Kercher et al., 2009) and the identical instrument described in Lopez-Hilfiker et al. (2012).

2.3 Determination of $\gamma(N_2O_5)$

N_2O_5 and the conditioned aerosol interacted within a pyrex, halocarbon wax-coated flow tube with an inner diameter (ID) of 3 or 6 cm and a length of 90 cm. Measurements were limited to the central 60 cm to maintain well-mixed, laminar flow conditions (Reynolds number = 106 or 53 depending on the flow tube diameter). The injector was moved to the top and bottom of the flow tube, altering the interaction time between N_2O_5 and the generated particles. The first-order rate loss (k_{het}) was determined using a pseudo-particle modulation technique (Bertram and Thornton, 2009):

$$k_{het} = -\left(\frac{1}{t_{res}}\right)\ln\left(\frac{[N_2O_5]_{top}}{[N_2O_5]_{bottom}}\right). \quad (1)$$

t_{res} is the resulting interaction time between the gases and particles. Wall losses of N_2O_5 to the flow tube (k_{wall}) were determined for each experiment in the same manner as k_{het} except in the absence of particles. The uptake efficiency, $\gamma(N_2O_5)$, was then determined from the equation

$$\gamma(N_2O_5) \approx \frac{4(k_{het} - k_{wall})}{\omega S_a}. \quad (2)$$
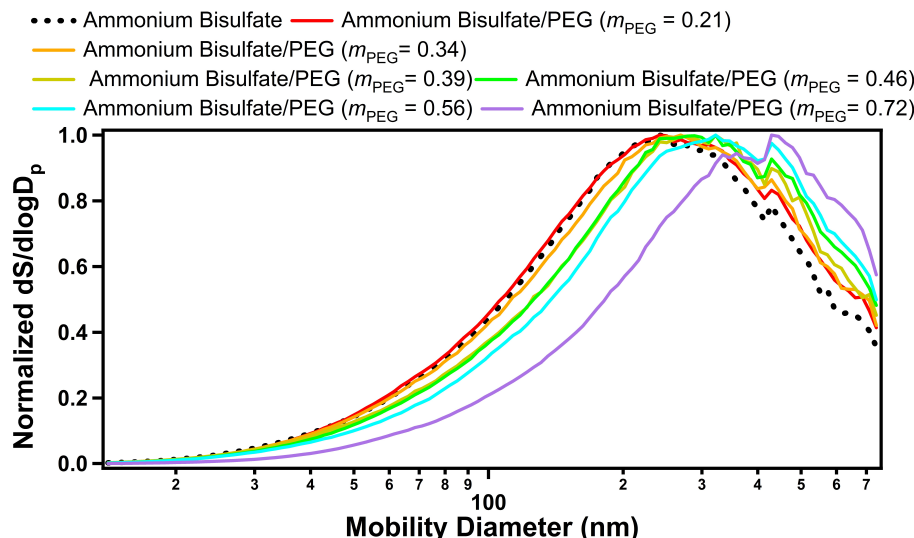
Figure 2. Representative surface area-weighted size distributions for ammonium bisulfate (black dotted line) and Ammonium Bisulfate/PEG aerosols generated from solutions with increasing mass (mole) fractions of PEG (colored lines).

ω represents the mean molecular velocity of N_2O_5 (Bertram and Thornton, 2009; McNeill et al., 2006; Riedel et al., 2012). Representative decays using this method are shown in Fig. S1 of the Supplement. This equation neglects gas-phase diffusion limitations to reactive uptake, which are small ($<10\%$) for the typical $\gamma(N_2O_5)$ and particle sizes used here (Fuchs and Sutugin, 1971). The $\gamma(N_2O_5)$ reported here are the mean of five independent determinations and the quoted uncertainties are the respective 95 % confidence intervals. Most $\gamma(N_2O_5)$ measurements are shown normalized to that measured on ammonium bisulfate at 50 % RH, which varied between 0.036 and 0.030, for comparison to other ambient and chamber data sets (Anttila et al., 2006; Bertram et al., 2009; Escorcia et al., 2010), and to account for drifts in sources of systematic errors related to flow rates, SMPS transmission and humidification, and CIMS detection efficiency. Moreover, the relative trends in $\gamma(N_2O_5)$ as a function of RH, χ_{OA}, and oxidation state are the primary focus of these measurements. Normalized measured values of $\gamma(N_2O_5)$ for all experiments are summarized in Table 1; absolute values can be obtained by multiplying the normalized values by the absolute $\gamma(N_2O_5)$ for ammonium bisulfate.

3 Results and discussion

3.1 Ammonium bisulfate and PEG experiments: evidence for the role of liquid–liquid phase separations

Figure 3a shows $\gamma(N_2O_5)$ measured on pure PEG particles vs. RH. The $\gamma(N_2O_5)$ increased with particle water content from 0.003 ± 0.003 at 30 % RH, 0.007 ± 0.003 at 50 % RH, to 0.017 ± 0.011 at 70 % RH. These values start approxi-

mately a factor of 10 lower than that for ammonium bisulfate particles and with increasing RH reach a value that is a factor of 2 lower than ammonium bisulfate, suggesting an additional limitation to reactive uptake of N_2O_5 on PEG compared to ammonium bisulfate. Also shown in Fig. 3a are predicted values of $\gamma(N_2O_5)$ derived from the model of Bertram and Thornton (2009) (see black dashed line), which uses the particulate water, nitrate, and chloride content in addition to the total particle volume and surface area to predict $\gamma(N_2O_5)$; the model assumes that N_2O_5 reacts throughout the bulk of the particle without any additional solubility or diffusion limitations compared to pure water. The water content of the PEG particles was calculated with the AIM II model and using the ethylene oxide (CH_2OCH_2) and the hydroxyl (OH) functional groups in UNIFAC, which has been previously shown to predict accurately the water activity of PEG solutions (Marcolli and Peter, 2005; Ninni et al., 1999; Ninni et al., 2000). The predicted $\gamma(N_2O_5)$ values are within error of the measured values despite the fact that we assume the solubility and diffusivity of N_2O_5 in PEG is the same as that for aqueous inorganic solutions.

In Fig. 3b, we show normalized $\gamma(N_2O_5)$ measured on particles that are mixtures of ammonium bisulfate and PEG (labeled Ammonium Bisulfate/PEG from here). At 50 % RH, the $\gamma(N_2O_5)$ decreased nearly linearly from the ammonium bisulfate value as the PEG mass fraction increased until a PEG mass fraction of ~ 0.6, beyond which the normalized $\gamma(N_2O_5)$ plateaued at ~ 0.20. As shown in Fig. 4, using particles with a PEG mass fraction of 0.2, where only minimal suppression of reactivity was observed at RH $= 50$ %, and decreasing the RH from 50 to 30 % resulted in a 70 % decrease in $\gamma(N_2O_5)$. In contrast, using particles with a PEG mass fraction of 0.56, where significant suppression of reactivity

Table 1. Relative humidity (RH), solution types and weight percentages, organic mass fractions (χ_{OA}), organic molar ratios, and $\gamma(N_2O_5)$ values (both absolute and normalized). The stated uncertainty in both the absolute and normalized values of $\gamma(N_2O_5)$ are 95 % confidence intervals.

RH (%)	Solution type	Wt %	Components	χ_{OA}	Organic O : C ratio	$\gamma(N_2O_5)$	Normalized $\gamma(N_2O_5)$
50	1	0.085	Ammonium bisulfate	N/A	N/A	0.036 ± 0.002	1.00 ± 0.058
30	1	0.300	PEG	1.000	0.56	0.003 ± 0.003	0.08 ± 0.07
50	1	0.300	PEG	1.000	0.56	0.007 ± 0.003	0.20 ± 0.07
70	1	0.300	PEG	1.000	0.56	0.017 ± 0.011	0.47 ± 0.30
30	2	0.107	Ammonium bisulfate + PEG	0.210	0.56	$0.009 \pm 6.5e\text{-}4$	0.24 ± 0.02
50	2	0.107	Ammonium bisulfate + PEG	0.210	0.56	0.028 ± 0.002	0.77 ± 0.04
50	2	0.129	Ammonium bisulfate + PEG	0.340	0.56	0.017 ± 0.004	0.47 ± 0.10
50	2	0.140	Ammonium bisulfate + PEG	0.390	0.56	0.016 ± 0.002	0.45 ± 0.05
50	2	0.159	Ammonium bisulfate + PEG	0.460	0.56	0.011 ± 0.002	0.31 ± 0.05
50	2	0.195	Ammonium bisulfate + PEG	0.560	0.56	0.004 ± 0.006	0.12 ± 0.17
70	2	0.195	Ammonium bisulfate + PEG	0.560	0.56	0.023 ± 0.003	0.62 ± 0.08
50	2	0.306	Ammonium bisulfate + PEG	0.720	0.56	$0.007 \pm 8.0e\text{-}4$	0.20 ± 0.02
50	2	0.092	Ammonium bisulfate + azelaic acid	0.076	0.44	0.023 ± 0.006	0.64 ± 0.17
30	2	0.099	Ammonium bisulfate + azelaic acid	0.140	0.44	0.004 ± 0.005	0.10 ± 0.12
50	2	0.099	Ammonium bisulfate + azelaic acid	0.140	0.44	0.019 ± 0.004	0.52 ± 0.10
50	2	0.113	Ammonium bisulfate + azelaic acid	0.250	0.44	0.017 ± 0.007	0.48 ± 0.18
50	2	0.131	Ammonium bisulfate + azelaic acid	0.350	0.44	0.012 ± 0.001	0.33 ± 0.04
50	2	0.154	Ammonium bisulfate + azelaic acid	0.450	0.44	0.010 ± 0.005	0.27 ± 0.13
70	2	0.154	Ammonium bisulfate + azelaic aid	0.450	0.44	0.016 ± 0.003	0.44 ± 0.07
50	2	0.215	Ammonium bisulfate + azelaic acid	0.620	0.44	0.007 ± 0.005	0.20 ± 0.13
50	2	0.363	Ammonium bisulfate + azelaic acid	0.760	0.44	0.008 ± 0.002	0.21 ± 0.04
30	2	0.094	Ammonium bisulfate + succinic acid	0.097	1.0	0.019 ± 0.007	0.42 ± 0.16
50	2	0.094	Ammonium bisulfate + succinic acid	0.093	1.0	0.045 ± 0.016	1.00 ± 0.35
50	2	0.102	Ammonium bisulfate + succinic acid	0.170	1.0	0.035 ± 0.006	0.78 ± 0.14
50	2	0.114	Ammonium bisulfate + succinic acid	0.254	1.0	0.037 ± 0.018	0.81 ± 0.41
50	2	0.129	Ammonium bisulfate + succinic acid	0.340	1.0	0.036 ± 0.007	0.80 ± 0.15
70	2	0.129	Ammonium bisulfate + succinic acid	0.340	1.0	0.040 ± 0.003	0.89 ± 0.06
50	2	0.172	Ammonium bisulfate + succinic acid	0.500	1.0	0.036 ± 0.003	0.79 ± 0.06
50	2	0.260	Ammonium bisulfate + succinic acid	0.670	1.0	0.026 ± 0.003	0.58 ± 0.06
30	2	0.099	Ammonium bisulfate + citric acid	0.146	1.17	0.011 ± 0.006	0.30 ± 0.15
50	2	0.099	Ammonium bisulfate + citric acid	0.146	1.17	0.025 ± 0.011	0.70 ± 0.31
50	2	0.113	Ammonium bisulfate + citric acid	0.250	1.17	0.024 ± 0.005	0.65 ± 0.14
50	2	0.132	Ammonium bisulfate + citric acid	0.360	1.17	0.019 ± 0.005	0.51 ± 0.13
50	2	0.156	Ammonium bisulfate + citric acid	0.450	1.17	0.013 ± 0.005	0.35 ± 0.14
70	2	0.156	Ammonium bisulfate + citric acid	0.450	1.17	0.035 ± 0.002	0.95 ± 0.05
50	2	0.226	Ammonium bisulfate + citric acid	0.620	1.17	0.017 ± 0.005	0.46 ± 0.14
50	2	0.370	Ammonium bisulfate + citric acid	0.770	1.17	0.013 ± 0.003	0.37 ± 0.08
50	1	0.085	Ammonium bisulfate	N/A	N/A	0.030 ± 0.005	1.00 ± 0.15
50	2	0.183	Ammonium bisulfate + glutaric acid	0.530	0.8	0.018 ± 0.003	0.6 ± 0.11
50	2	0.162	Ammonium bisulfate + malonic acid	0.470	1.33	0.021 ± 0.003	0.68 ± 0.09
30	3	0.089	Ammonium bisulfate + high O / C (glucose, malonic acid, citric acid, succinic acid)	0.120	1.13	0.013 ± 0.006	0.42 ± 0.21
50	3	0.089	Ammonium bisulfate + high O / C	0.120	1.13	0.021 ± 0.003	0.71 ± 0.11
50	3	0.122	Ammonium bisulfate + high O / C	0.300	1.13	0.017 ± 0.004	0.57 ± 0.12
50	3	0.195	Ammonium bisulfate + high O / C	0.559	1.13	0.010 ± 0.002	0.33 ± 0.05
70	3	0.195	Ammonium bisulfate + high O / C	0.559	1.13	0.015 ± 0.003	0.50 ± 0.10
50	3	0.110	Ammonium bisulfate + high O / C	1.000	1.13	0.005 ± 0.001	0.16 ± 0.04
30	3	0.091	Ammonium bisulfate + low O / C (azelaic acid, PEG, gentisic acid, (1,2,9)-nonanetriol)	0.156	0.48	0.003 ± 0.002	0.10 ± 0.06
50	3	0.091	Ammonium bisulfate + low O / C	0.156	0.48	0.008 ± 0.002	0.27 ± 0.08
50	3	0.135	Ammonium bisulfate + low O / C	0.370	0.48	0.007 ± 0.003	0.23 ± 0.10
50	3	0.236	Ammonium bisulfate + low O / C	0.635	0.48	0.006 ± 0.001	0.20 ± 0.03
70	3	0.236	Ammonium bisulfate + low O / C	0.635	0.48	0.013 ± 0.004	0.44 ± 0.13
50	3	0.151	Ammonium bisulfate + low O / C	1.000	0.48	0.002 ± 0.002	0.08 ± 0.06

was observed at RH = 50 %, and increasing the RH from 50 to 70 % led to a factor of 5 increase in $\gamma(N_2O_5)$. Both of these sensitivities to RH are far stronger than that of pure ammonium bisulfate (Bertram and Thornton, 2009). Also shown in Fig. 3b are the predicted values of $\gamma(N_2O_5)$ obtained from the Bertram and Thornton (2009) parameterization (black dashed line), assuming the particles are homogeneous (single-phase) internal mixtures, and allowing the PEG to partition between aqueous and hydrophobic phases in the AIM II model. The predicted values capture the measured $\gamma(N_2O_5)$ well for the two extremes, where the particles are composed of either 100 % ammonium bisulfate or 100 % PEG. However, the model fails to capture the observed behavior of $\gamma(N_2O_5)$ on Ammonium Bisulfate/PEG particles, likely because the model does not account for organic coatings formed due to liquid–liquid phase separations, which
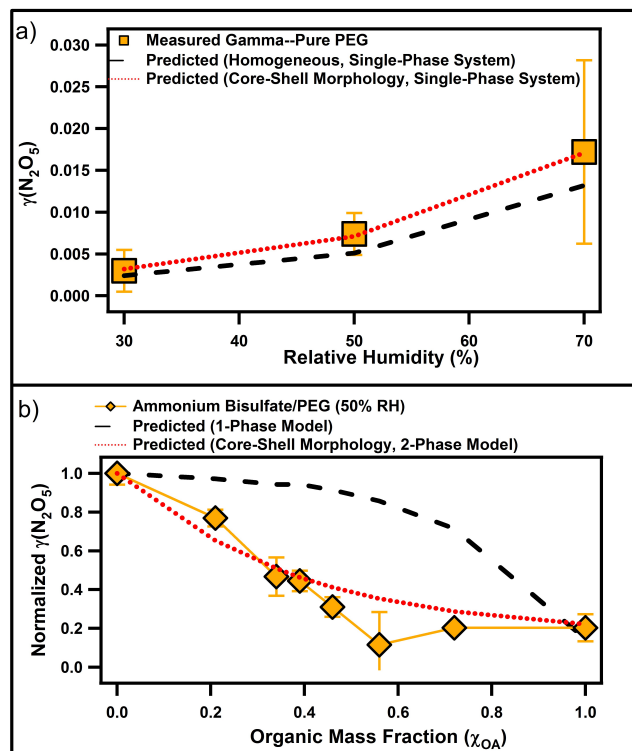
Figure 3. (a) Experimentally measured $\gamma(N_2O_5)$ values of pure PEG at 30 %, 50 %, and 70 % relative humidity (RH) (orange squares). (b) Experimentally measured normalized $\gamma(N_2O_5)$ values of particles generated from ammonium bisulfate and PEG as a function of PEG mass fraction at 50 % RH (orange diamonds connected by orange line). Predicted values of $\gamma(N_2O_5)$ for pure PEG (top panel) and for Ammonium Bisulfate/PEG particles (bottom panel) using the parameterizations of Bertram and Thornton (2009) (dashed black lines) and Anttila et al. (2006) (dashed red lines) are also shown.

have been shown to occur in mixtures of PEG and ammonium sulfate (Ciobanu et al., 2009; Marcolli and Krieger, 2006).

To investigate the role of particle morphology in N_2O_5 uptake, a slightly modified version of the core-shell resistivity model of Anttila et al. (2006) was also used to predict experimental results presented herein with the following equation:

$$\frac{1}{\gamma} = \frac{\omega R_p}{4 D_{gas}} + \frac{1}{\alpha} + \frac{\omega R_p}{4 R T H_{org} D_{org}(q_{org} F - 1)} \quad (3)$$

R_p is the particle radius (m), D_{gas} is the gas phase diffusion coefficient for N_2O_5 taken to be 1×10^{-5} m^2 s^{-1} (Anttila et al., 2006), α is the dimensionless mass accommodation coefficient, H_{org} is the Henry's law coefficient for N_2O_5 in the organic layer (mol/m^3 atm), D_{org} is the diffusion coefficient of N_2O_5 in the organic layer (m^2 s^{-1}), and q_{org} is the dimensionless diffuso-reactive parameter, which describes the competition between diffusion and reaction in the organic
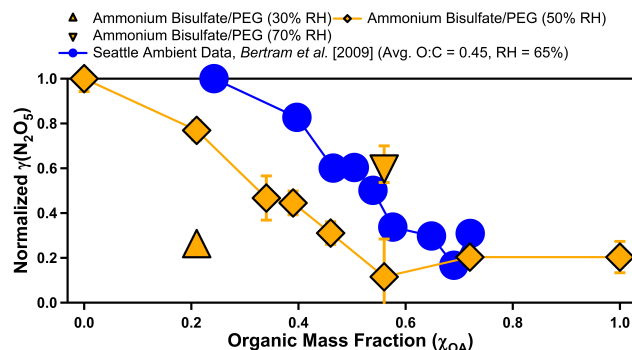
Figure 4. Normalized $\gamma(N_2O_5)$ values of particles generated from Ammonium Bisulfate/PEG as a function of PEG mass fraction at 30 % RH (orange, right-side-up triangle), 50 % RH (orange diamonds connected by orange line), and 70 % RH (orange upside-down triangle). Normalized $\gamma(N_2O_5)$ for ambient particles measured in Seattle, WA during the summer of 2008 (Bertram et al., 2009b) are also shown (blue dots connected by blue line). The average RH in the sampling inlet was 65 % RH and the average O:C ratio of the ambient organic aerosol was 0.45, estimated from an AMS operated simultaneously.

layer

$$q_{org} = R_p \sqrt{\frac{k_{org}}{D_{org}}}, \quad (4)$$

where k_{org} is the pseudo first-order reaction rate constant of N_2O_5 in the organic layer (s^{-1}). The equation for parameter F is given in Eq. (5):

$$F = \frac{\coth(q_{org}) + h(q_{aq}, q_{org}^*)}{1 + \coth(q_{aq}) h(q_{aq}, q_{org}^*)}. \quad (5)$$

The parameter F also contains the dimensionless diffuso-reactive parameter in the aqueous core of the particle (q_{aq}) similar to q_{org}; however, the reaction rate constant of N_2O_5 in the aqueous layer (k_{aq}) and the diffusion coefficient in the aqueous core (D_{aq}) are used instead. The model of Anttila et al. (2006) considers k_{aq} a tunable parameter; however, the model of Bertram and Thornton (2009) explicitly parameterizes the equivalent rate constant (k_{2f}') as a function of liquid water, nitrate, and chloride content using the RH and inorganic composition of the particle in the AIM II model. We therefore use the Bertram and Thornton parameterization for k_{aq} to capture the dependence of $\gamma(N_2O_5)$ on the liquid water better. Further information regarding the model of Anttila et al. (2006) and the equations used can be found in the Supplement. We note that this parameterization does not factor in temperature dependencies of $\gamma(N_2O_5)$, which may also be important (Abbatt et al., 2012; Wagner et al., 2013).

The water activity and diffusivity of PEG solutions are reasonably well constrained by independent data, and thus the Ammonium Bisulfate/PEG particles provide a useful test

case for the reactive uptake model. Table 2 shows the values of each variable used in the model of Anttila et al. (2006) for PEG and mixtures of Ammonium Bisulfate/PEG. The N_2O_5 rate constant in the organic coating (k_{org}) for pure PEG particles was determined to be $2.0 \times 10^5 \, \mathrm{s}^{-1}$ at 50 % RH, increasing by a factor of ~ 1.6 to $3.2 \times 10^5 \, \mathrm{s}^{-1}$ as the RH was increased to 70 %, and decreasing by a factor of ~ 3 to $7.0 \times 10^4 \, \mathrm{s}^{-1}$ as the RH was decreased to 30 %. Values of k_{org} can be used to probe the particle liquid water content assuming that k_{org} is equivalent to the rate constant of N_2O_5 in water derived from Bertram and Thornton (2009) (k'_{2f}) multiplied by the liquid water content in the PEG. The liquid water content of PEG predicted using the values of k_{org} at each RH matched the predicted liquid water content using the AIM II model to within 40 % or better at all RHs, suggesting that N_2O_5 uptake kinetics can provide an additional metric to assess the liquid water content of both inorganic and organic aerosol. In addition to k_{org}, ε, the factor used to scale the product of D_{aq} and H_{aq} to account for the decrease in diffusion and solubility of N_2O_5 in the organic layer compared to the aqueous core, was also found to be important for achieving agreement between experimental and predicted values. The best agreement was found by setting $\varepsilon = 0.06$ for Ammonium Bisulfate/PEG at 30 % RH, $\varepsilon = 0.3$ at 50 % RH, and $\varepsilon = 1$ at 70 % RH. Using the constraints from the observed dependence of $\gamma(N_2O_5)$ on the PEG mass fraction, and the model sensitivity to q_{org}, we conclude that the changes in ε represent mostly changes in D_{org} relative to D_{aq} and less so changes in H_{org} compared to H_{aq} (see Supplement), a finding similar to Antilla et al. (2006). Assuming that the largest changes in $\gamma(N_2O_5)$ Ammonium Bisulfate/PEG particles compared to ammonium bisulfate particles are driven by changes in diffusivity and reactivity, we find the best model–measurement agreement with $D_{org} = 3$ to $5 \times 10^{-10} \, \mathrm{m^2 \, s^{-1}}$ at 50 % RH. For comparison, assuming the PEG mass fraction in pure PEG particles is ~ 0.85 at 50 % RH (Ninni et al., 1999) and using an estimated dynamic viscosity of $\sim 14.7 \, \mathrm{mPa \, s^{-1}}$ (Rahbari-Sisakht et al., 2003) for PEG-300 yields a value of D_{org} of $\sim 10^{-10} \, \mathrm{m^2 \, s^{-1}}$ using the Stokes–Einstein equation. At 70 % RH, best agreement between the observed $\gamma(N_2O_5)$ and that predicted by the resistor model was obtained when D_{org} was equal to D_{aq} ($1 \times 10^{-9} \, \mathrm{m^2 \, s^{-1}}$) and $H_{org} = H_{aq}$ for both pure PEG and Ammonium Bisulfate/PEG particles, suggesting the presence of internally mixed systems at this higher RH and the lack of phase separations.

The modified Antilla et al. (2006) resistor model predictions of $\gamma(N_2O_5)$ generally match measured values for both pure PEG (assuming a single-phase system) and mixtures of Ammonium Bisulfate/PEG (assuming a two-phase system); see Fig. 3a and b. As noted above, the parameterization of Bertram and Thornton (2009) also achieved good agreement for pure PEG particles despite the fact that it does not account for diffusion limitations of N_2O_5 in PEG. Bertram and Thornton (2009) use a lower value for H_{aq} than Anttila et

al. (2006), while Anttila et al. (2006) use a lower value for D_{org} than that used by Bertram and Thornton (2009), who conclude that the diffusion limitation in aqueous solution particles was negligible. These differing values of H_{aq} likely cancel the effects of the different approaches to diffusion limitations. Thus, while there is good agreement between both models and measured values of $\gamma(N_2O_5)$ for pure PEG, the two models are not directly comparable as they are based on different assumptions. In contrast, for Ammonium Bisulfate/PEG mixtures, the model of Anttila et al. (2006) clearly predicts values of $\gamma(N_2O_5)$ with much higher accuracy than that of Bertram and Thornton (2009), likely due to the fact that only modest decreases in the overall liquid water content of mixed Ammonium Bisulfate/PEG particles are predicted for an internally mixed system; however, these modest decreases in liquid water content cannot fully explain the behavior of $\gamma(N_2O_5)$. Instead, the formation of organic coatings of PEG through liquid–liquid phase separations likely further decreases the liquid water content in the coating and additional decreases in N_2O_5 solubility and diffusivity in a coating of PEG likely impact $\gamma(N_2O_5)$ as well; these decreases are more accurately represented by the core-shell resistivity model of Anttila et al. (2006).

We conclude this section by noting that $\gamma(N_2O_5)$ on Ammonium Bisulfate/PEG particles show strikingly similar dependencies on χ_{OA} to $\gamma(N_2O_5)$ measured on ambient atmospheric particles (Bertram et al., 2009), as shown in Fig. 4. We note that the χ_{OA} in the ambient particles is mostly secondary in nature (e.g., most of the organic aerosol is oxidized organic aerosol, OOA) (Bertram et al., 2009). In both the laboratory and field measurements, a similar nearly linear decrease in $\gamma(N_2O_5)$ with increasing χ_{OA} was observed, with linear fits to the normalized $\gamma(N_2O_5)$ vs. χ_{OA} having slopes of -1.6 and -1.7, respectively (see Fig. S2 in the Supplement). Due to the similar response of the normalized $\gamma(N_2O_5)$ to increases in χ_{OA}, a comparison of these two systems was made. The O : C of PEG-300 is 0.56, while the average O : C of the χ_{OA} in the ambient particles was estimated to be ~ 0.45 as measured by an Aerodyne aerosol mass spectrometer (AMS) with unit-mass resolution (see Fig. S3 and Supplement for this calculation). However, this latter value may be an under-estimate as recent measurements have shown the AMS can under-predict O : C by up to $\sim 25 \%$; this observation holds for both the unit-mass resolution and high-resolution AMS (Canagaratna, 2014). Furthermore, the average RH during ambient sampling conditions was 65 %, which is higher than most of the Ammonium Bisulfate/PEG experiments that were primarily conducted at 50 % RH. At 70 % RH, $\gamma(N_2O_5)$ on Ammonium Bisulfate/PEG particles were found roughly to match $\gamma(N_2O_5)$ on ambient particles with similar χ_{OA}.

There are several possible ways to explain why laboratory measurements of N_2O_5 uptake onto particles composed of ammonium bisulfate and PEG mimic uptake experiments on ambient aerosol so well. First, the polymeric nature of PEG

Table 2. Input parameters for the model of Anttila et al. (2006) used to predict $\gamma(N_2O_5)$.

RH	Compound	α	$[H_2O]_{ABS}$	k_{aq} (k_{2f})	k_{org}	ε	D_{org}
50 %	Ammonium bisulfate	0.1	25.7	1.11×10^6	0.00E+00	1.00	1.00×10^{-9}
30 %	PEG	0.1	13.6	9.50×10^5	7.00×10^4	0.06	6.00×10^{-11}
50 %	PEG	0.1	25.7	1.11×10^6	2.00×10^5	0.30	5.00×10^{-10}
70 %	PEG	0.1	36.5	1.14×10^6	3.20×10^5	1.00	1.00×10^{-9}
30 %	Ammonium Bisulfate/PEG	0.1	13.6	9.50×10^5	7.00×10^4	0.06	6.00×10^{-11}
50 %	Ammonium Bisulfate/PEG	0.1	25.7	1.11×10^6	2.00×10^5	0.30	5.00×10^{-10}
70 %	Ammonium Bisulfate/PEG	0.1	36.5	1.14×10^6	3.20×10^5	1.00	1.00×10^{-9}
30 %	Ammonium bisulfate/low OC	0.1	13.6	9.50×10^5	1.23×10^4	0.008	8.00×10^{-12}
50 %	Ammonium bisulfate/low OC	0.1	25.7	1.11×10^6	3.50×10^4	0.05	5.00×10^{-11}
70 %	Ammonium bisulfate/low OC	0.1	36.5	1.14×10^6	5.60×10^4	0.80	1.00×10^{-9}
30 %	Ammonium bisulfate/high OC	0.1	13.6	9.50×10^5	7.00×10^4	0.06	5.00×10^{-10}
50 %	Ammonium bisulfate/high OC	0.1	25.7	1.11×10^6	2.00×10^5	0.30	1.00×10^{-9}
70 %	Ammonium bisulfate/high OC	0.1	36.5	1.14×10^6	3.20×10^5	0.80	1.00×10^{-9}

may be similar to SOA found in ambient aerosols, which have been found to contain oligomers in certain environments (Denkenberger et al., 2007; Kalberer et al., 2004; Surratt et al., 2006); however, the presence of liquid–liquid phase separations is an additional possibility. While speculative, the similar behavior of $\gamma(N_2O_5)$ observed on Ammonium Bisulfate/PEG mixtures, which are known to exhibit liquid–liquid phase separations (Ciobanu et al., 2009; Marcolli and Krieger, 2006), and on ambient aerosol is certainly consistent with the idea that ambient organic aerosol constituents undergo humidity-dependent liquid–liquid phase separations, thereby inhibiting heterogeneous losses of N_2O_5.
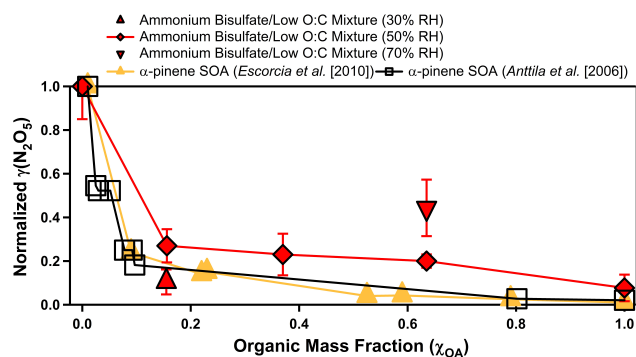
3.2 Ammonium bisulfate and organic compounds with low O : C

N_2O_5 uptake onto mixtures of ammonium bisulfate and organic compounds with low O : C ratios (mean O : C ratio = 0.48 for the mixture) as a function of χ_{OA} is shown in Fig. 5; a mixture of several organic components, including organic acids and polyols, was used to minimize the chance of crystallization (Marcolli et al., 2004). In contrast to the experiments using organics with a high O : C ratio described below, $\gamma(N_2O_5)$ decreased by ~ 70–80 % with an χ_{OA} of as little as ~ 15 %, beyond which $\gamma(N_2O_5)$ remained at a nearly constant suppressed value. Similar trends in $\gamma(N_2O_5)$ were found for mixtures of ammonium bisulfate and azelaic acid only (see Fig. S4 in the Supplement). Azelaic acid, one of the components used in the low O : C mixture that has the same O : C ratio as the mixture, has been shown to exhibit a salting out effect in the presence of inorganic salts (Reid et al., 2011). Observations of a rapid decrease in $\gamma(N_2O_5)$ with small amounts of organics are in agreement with previous laboratory studies using surface-active compounds (McNeill

et al., 2006; Thornton and Abbatt, 2005), humic acids (Badger et al., 2006), and secondary organic aerosol (SOA) from α-pinene ozonolysis (Anttila et al., 2006; Escorcia et al., 2010; Folkers et al., 2003). Chemical measurements using an AMS suggest that SOA from α-pinene ozonolysis has an O : C ratio similar to that of semi-volatile oxygenated organic aerosol (SV-OOA, O : C = 0.35 ± 0.14) (Ng et al., 2010). As noted previously, this O : C ratio may be biased low by up to ~ 25 % (Canagaratna, 2014). As shown in Fig. 5, the changes in $\gamma(N_2O_5)$ we observe with the low O : C mixture were similar to, though somewhat smaller than, that measured using α-pinene ozonolysis SOA deposited on ammonium sulfate seed particles (Anttila et al., 2006; Escorcia et al., 2010; Folkers et al., 2003), suggesting our low O : C ratio mixture mimics the properties of α-pinene ozonolysis SOA that affect N_2O_5 reactive uptake. The similarity between the two systems could be due to similarities in the O : C ratios for the two systems, particularly if the correction to the AMS-derived O : C ratio is taken into account, or due to other similarities between the two systems, such as the properties of the polyols and organic acids found in our low O : C mixture.

Also shown in Fig. 5 are normalized $\gamma(N_2O_5)$ measurements at 30 % RH and 70 % RH with χ_{OA} of ~ 15.6 % and ~ 63.5 %, respectively. Normalized values of $\gamma(N_2O_5)$ are nearly a factor of 3 lower at 30 % RH, and coincidentally match N_2O_5 uptake onto chamber-derived biogenic SOA. This sensitivity to lower RH is far larger than for pure ammonium bisulfate (Bertram and Thornton, 2009), and, given the relatively small χ_{OA} (15 %), again suggests the presence of an organic coating having a different hygroscopicity (and thus water content) and viscosity than pure ammonium bisulfate. Increasing RH from 50 % to 70 % leads to more than a doubling of the $\gamma(N_2O_5)$, though it remains suppressed
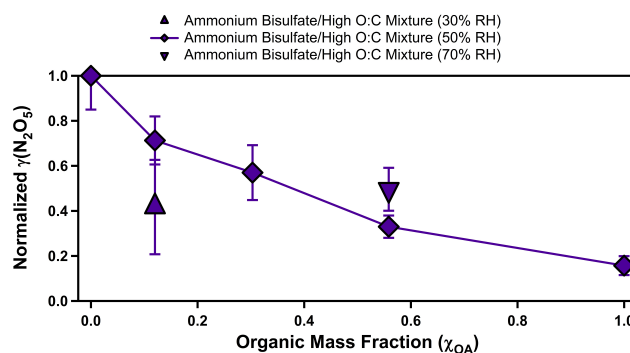
Figure 5. Normalized $\gamma(N_2O_5)$ values for particles generated from ammonium bisulfate and a mixture of organic compounds with a low O : C ratio as a function of χ_{OA} at 30 % RH (red, right-side-up triangle), 50 % RH (red diamonds connected by red line), and 70 % RH (red upside-down triangle). Normalized $\gamma(N_2O_5)$ for particles containing chamber-derived SOA from α-pinene oxidation as measured by Escorcia et al. (2010) (solid, orange triangles with connecting line) and reported by Anttila et al. (2006) (open, black squares with connecting line) are also shown.

compared to pure ammonium bisulfate particles by more than a factor of 2.

3.3 Ammonium bisulfate and organic compounds with high O : C

The uptake of N_2O_5 onto mixtures of ammonium bisulfate and organic compounds with high O : C ratios (mean O : C ratio = 1.13 for the mixture) as a function of RH and χ_{OA} is shown in Fig. 6. The normalized $\gamma(N_2O_5)$ decreased nearly linearly as the χ_{OA} increased, but this decrease (slope of -0.78; see Fig. S5 in the Supplement) was modest compared to the other systems investigated (e.g., ammonium bisulfate/low O : C mixtures and Ammonium Bisulfate/PEG). As shown in Fig. 6, at an χ_{OA} of 10 %, decreasing the RH from 50 to 30 % leads to a 40 % decrease in $\gamma(N_2O_5)$, less of an RH dependence compared to the ammonium bisulfate/low O : C mixture, but stronger than that for pure ammonium bisulfate (Bertram and Thornton, 2009). At an χ_{OA} of 56 %, increasing RH from 50 % to 70 % leads to a 33 % increase in $\gamma(N_2O_5)$, again less than for the ammonium bisulfate/low O : C mixture.

Previous measurements have shown that water soluble organic carbon is likely to have a high O : C ratio (Duong et al., 2011), and that higher O : C organic aerosol has higher hygroscopicity (Jimenez et al., 2009). Thus, these more modest decreases in $\gamma(N_2O_5)$ with increasing organic mass fraction likely indicate that appreciable water content and/or fewer diffusion limitations are associated with organics with a higher O : C ratio compared to those with lower O : C ratios. Further, these modest decreases in $\gamma(N_2O_5)$ compared to those measured on ammonium bisulfate particles are in line with previous measurements of $\gamma(N_2O_5)$
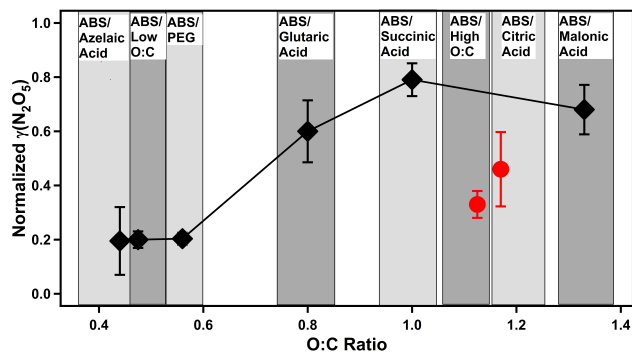

Figure 6. Normalized $\gamma(N_2O_5)$ values for particles generated from ammonium bisulfate and a mixture of organic compounds with a high O : C ratio as a function of χ_{OA} at 30 % RH (purple, right-side-up triangle), 50 % RH (purple diamonds connected by purple line), and 70 % RH (purple upside-down triangle).

on particles composed of dicarboxylic acids having O : C ratios of 0.8–2 (Griffiths et al., 2009; Thornton et al., 2003). We found significant differences in $\gamma(N_2O_5)$ when using mixtures of ammonium bisulfate and individual high O : C organic components. For example, $\gamma(N_2O_5)$ on particles composed of ammonium bisulfate and succinic acid alone showed little change with increasing succinic acid mass fraction (see Fig. S6 in the Supplement). In contrast, decreases in $\gamma(N_2O_5)$ were observed for mixtures of ammonium bisulfate and citric acid alone that were similar to the decrease observed using the high O : C mixture (see Fig. S7 in the Supplement). Citric acid was one of the components used in the high O : C mixture, representing 32 % of the organic mass, that has the same O : C ratio as the mixture, and may be responsible for the decrease in N_2O_5 uptake with an increasing mass fraction of the high O : C mixture used here. Both citric acid and glucose can form amorphous phases, which may also play a role in the observed dependence of normalized $\gamma(N_2O_5)$ on the χ_{OA} (Koop et al., 2011). These results illustrate the challenge associated with faithfully reproducing the properties of atmospheric organic aerosol using individual compounds.

3.4 Role of Organic O : C ratio on $\gamma(N_2O_5)$

Figure 7 shows normalized $\gamma(N_2O_5)$ vs. the O : C ratio of particles that are mixtures of organic components and ammonium bisulfate. The response at a single organic mole fraction of 0.5 is shown; more data points were taken at this mole fraction, and the effect of the O : C ratio on $\gamma(N_2O_5)$ at different mole fractions was similar, albeit weaker. Because the carbon oxidation state followed the same trend as the organic O : C ratio, only the dependence of $\gamma(N_2O_5)$ on the O : C ratio is shown. In addition to PEG, low O : C and high O : C mixtures, $\gamma(N_2O_5)$ on particles that are two-component mixtures of ammonium bisulfate and azelaic, glutaric, succinic, citric, or malonic acids are also shown. For organics with
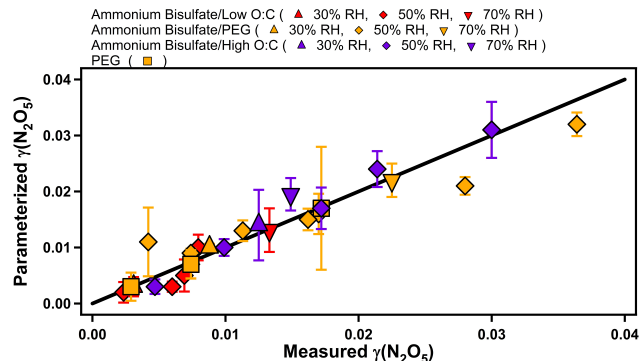
Figure 7. Normalized $\gamma(N_2O_5)$ values for ammonium bisulfate (denoted as ABS in this figure) and organic mixtures as a function of an organic O : C ratio at an organic mole fraction of 0.5 and RH of 50 % (black markers). Red markers denote values for mixtures of ammonium bisulfate (ABS) and citric acid and ammonium bisulfate (ABS) and the high O : C mixture.

Figure 8. Measured $\gamma(N_2O_5)$ and parameterized $\gamma(N_2O_5)$ using the model of Anttila et al. (2006) for particles composed of an ammonium bisulfate + low O : C organic mixture (red markers), ammonium bisulfate + PEG (orange markers), pure PEG (orange squares), and an ammonium bisulfate + high O : C organic mixture (purple markers) at all χ_{OA}. Values at 30 % RH are shown as right-side-up triangles, those at 50 % RH are shown as diamonds, and those at 70 % RH are shown as upside-down triangles. The black line represents a 1 : 1 ratio between the measured and parameterized uptake values fit through the origin.

an O : C of ~ 0.45, significant suppression in N_2O_5 uptake occurs at low organic mole fractions (e.g., $\gamma(N_2O_5)$ drops by 70–80 % relative to pure ammonium bisulfate at organic mole fractions of only 0.1) with little changes observed after the initial suppression. In general, for organics with high O : C ratios (e.g., O : C > 0.7), relatively little suppression of $\gamma(N_2O_5)$ was observed. An unexpected result was the observation that mixtures of ammonium bisulfate with citric acid and with the high O : C mixture showed more suppression than mixtures of ammonium bisulfate with other organics having O : C > 0.7. As shown in Fig. 7, $\gamma(N_2O_5)$ increases as the O : C ratio increases above 0.56. Together with the different responses to RH exhibited by the lower O : C mixtures compared to the higher O : C, the dependence upon O : C observed here is consistent with the observation that liquid–liquid phase separations most readily occur for organic compounds with O : C ratios of ≤ 0.7 (Bertram et al., 2011; You et al., 2013) and RH < 70 %. However, our results also show that the O : C ratio is not the only controlling factor for the effect of organic components on $\gamma(N_2O_5)$. Moreover, even if phase separations occurred for all systems studied here, a dependence upon O : C is still expected due to its correlation with higher hygroscopicity and thus a greater water content within an organic phase that would promote N_2O_5 reactivity.

3.5 Model predictions of $\gamma(N_2O_5)$ for low and high O : C mixtures with ammonium bisulfate

In addition to the pure PEG and Ammonium Bisulfate/PEG mixtures described above, mixtures of ammonium bisulfate and other organics were also modeled using the modified version of the Anttila et al. (2006) resistor model of reactive uptake described above. Figure 8 shows a comparison of $\gamma(N_2O_5)$ measured from mixtures of ammonium bisulfate and organic compounds with different oxidation states vs. parameterized values. Although we cannot rule out the pos-

sibility of organic lenses (e.g., incomplete organic coatings) (Reid et al., 2011), for simplicity, we assume each particle is completely coated. This assumption is likely valid since predicted values of $\gamma(N_2O_5)$ obtained from the assumption of an organic lens were found to consistently over-predict the measured $\gamma(N_2O_5)$ with the possible exception of the high O : C mixture. For the core-shell model, excellent agreement (slope = 0.98, $R^2 = 0.91$) is found for all systems at all RH values used in this work. Table 2 shows the values of each model variable used. Predicted values of $\gamma(N_2O_5)$ were less sensitive to values of α, the mass accommodation coefficient, than for other parameters, in agreement with the findings of Anttila et al. (2006) and Riemer et al. (2009). The k_{org} required to bring observed and predicted $\gamma(N_2O_5)$ into agreement differed by more than an order of magnitude, ranging from 3.5×10^4 to 2×10^5 s^{-1} for the low O : C and high O : C mixtures, respectively, at 50 % RH.

For the high O : C mixture at both 50 % and 70 % RH, reasonable agreement was achieved by simply lowering k_{org} compared to k_{aq} and lowering ε from 1 to 0.3 without necessarily invoking any changes in the diffusivity of N_2O_5 in the organic layer suggesting that solubility limitations and differences in the liquid water content between the aqueous and organic components are primarily responsible for the behavior of $\gamma(N_2O_5)$ as a function of the organic content for the high O : C mixture. At 30 % RH, best agreement is achieved when D_{org} is lowered to half the value of D_{aq} for the high O : C mixture.

In contrast, poor agreement was observed for the low O : C mixture when only differences in the liquid water content (k_{org}) and solubility of N_2O_5 in the organic layer are

accounted for. Instead, better agreement is achieved when D_{org} is lowered to 5×10^{-11} m^2 s^{-1}, a value approaching a viscous liquid (Koop et al., 2011; Shiraiwa et al., 2011). At 70 % RH, best agreement was obtained when D_{org} was equal or close to D_{aq} (8×10^{-10} to 1×10^{-9} m^2 s^{-1}), suggesting the presence of internally mixed systems at this higher RH. At 50 % RH, the best agreement was found by setting $\varepsilon = 0.05$ for the ammonium bisulfate/low O : C mixture, which is similar to the value of $\varepsilon = 0.03$ used to achieve agreement between measured and predicted values of $\gamma(N_2O_5)$ onto biogenic SOA derived from α-pinene ozonolysis (Anttila et al., 2006; Riemer et al., 2009). Our results further support findings that suggest that changes in diffusion and/or solubility can result in large reductions in the N$_2$O$_5$ uptake efficiency, even for thin coatings, without having to invoke changes in α. The fact that ε is similar for the low O : C mixture used in this work and biogenic SOA suggests that similar diffusion limitations exist for these two systems.

4 Atmospheric implications and conclusions

Measured values of $\gamma(N_2O_5)$ were well predicted using a model that accounts for liquid–liquid phase separations into a core-shell morphology given suitable adjustments to the water content and N$_2$O$_5$ diffusivity and solubility within the organic shell. As expected, these parameters were dependent upon organic composition and humidity. Moreover, the dependence of $\gamma(N_2O_5)$ on χ_{OA} observed in these laboratory studies is remarkably similar to that observed on ambient aerosol particles, indicating that similar parameterizations could be used to predict $\gamma(N_2O_5)$ on ambient aerosol, at least in some cases. Below, we use these insights into the effects of organic aerosol mass fraction and composition on N$_2$O$_5$ developed in this work and field measurements of these quantities to illustrate the impact of organic aerosol on N$_2$O$_5$ reactivity.

4.1 Model predictions of $\gamma(N_2O_5)$ applied to ambient aerosol

We extend our predictions of $\gamma(N_2O_5)$ to ambient aerosol using global measurements of submicron, non-refractory aerosol composition using AMS ambient data sets. The O : C ratio was determined for 25 data sets ranging from urban to remote environments from f (fraction of m/z 44 to total organics in the mass spectrum) (Aiken et al., 2008; Ng et al., 2010); details of the data sets can be found in Jimenez et al. (2009) and the Supplement. To parameterize the impact of RH, the organic aerosol mass fraction (χ_{OA}), and the O : C ratio, we first model the impact of RH (e.g., liquid water content) on the $\gamma(N_2O_5)$ for pure ammonium bisulfate using the model of Bertram and Thornton (2009) (see Fig. 9, dashed black line). We then factor in the effect of
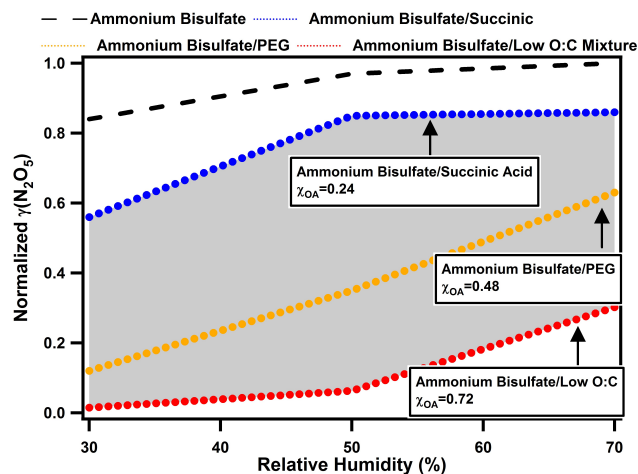
Figure 9. Predicted $\gamma(N_2O_5)$ for pure ammonium bisulfate (dashed black lines) as a function of RH, normalized to RH > 50 % values. The effect of organic aerosol on $\gamma(N_2O_5)$ under atmospheric conditions is shown using trends observed in this study and ambient organic aerosol abundance and composition obtained from AMS data sets. See text for details.

organic aerosol using the model of Anttila et al. (2006), the average χ_{OA} (0.48 ± 0.12), and the average O : C ratio (O : C $= 0.46 \pm 0.14$) determined from all 25 data sets. The average O : C ratio is low enough that liquid–liquid phase separations can potentially form, particularly at RH $\leq$ 70 % (Bertram et al., 2011; Renbaum-Wolff et al., 2013; Saukko et al., 2012). PEG was used as a model organic compound, which is appropriate when considering that the dependence of $\gamma(N_2O_5)$ on the mass fraction of PEG for Ammonium Bisulfate/PEG mixtures was found to resemble the dependence of $\gamma(N_2O_5)$ on the χ_{OA} exhibited by ambient aerosol that had a similar average O : C ratio (O : C $= 0.45$). The dotted orange line in Fig. 9 shows the impact of factoring in organic coatings using PEG as the model compound and the database average χ_{OA} (0.48). Compared to pure ammonium bisulfate, the normalized value of $\gamma(N_2O_5)$ was found to be lower by 40 % at 70 % RH, by 60 % at 50 % RH, and by 85 % at 30 % RH.

We also use 95 % confidence intervals, taken as two standard deviations, for the organic aerosol mass fraction and use organics that exhibit a wide range of influence on $\gamma(N_2O_5)$ (e.g., from near-complete suppression to almost no impact) to predict the range of different possible effects organic coatings will have on $\gamma(N_2O_5)$. For the case where the organic coating would have the largest impact on $\gamma(N_2O_5)$, we use the upper limit of the 95 % confidence interval for the typical χ_{OA}, which is 0.72, and an organic composition similar to the low O : C mixture, which suppressed $\gamma(N_2O_5)$ the most. The corresponding prediction for $\gamma(N_2O_5)$ is shown in Fig. 9 as a dotted red line; $\gamma(N_2O_5)$ decreases by an order of magnitude or more at 30 and 50 % RH. For the case where the organic coating would have a minimal effect on $\gamma(N_2O_5)$,

we use the lower limit of the 95 % confidence interval for the typical χ_{OA}, which is 0.24 from the database, and the ammonium bisulfate/succinic acid mixture. We choose succinic acid because, as shown in Fig. 7 and Table 1, even at a high χ_{OA}, succinic acid has a minimal impact on $\gamma(N_2O_5)$. The corresponding predictions of $\gamma(N_2O_5)$ are shown in Fig. 9 as a dotted blue line; $\gamma(N_2O_5)$ only decreases by ~ 33 % at 30 % RH and only by ~ 15 % at 50 and 70 % RH.

While the estimates of the impact of organics on $\gamma(N_2O_5)$ will depend on phase (e.g., whether an organic coating forms) in addition to coating thicknesses, particle surface area, and humidity, the predictions presented in Fig. 9 capture a uniformly suppressing effect of organic aerosol on N_2O_5 reactivity observed in previous studies (Bertram et al., 2009; Brown et al., 2009; Riedel et al., 2012) and illustrate that significant variability in the degree of suppression is expected. To the extent which averaging over multiple data sets from different regions and seasons yields a reasonable estimate of the "typical" organic aerosol, these calculations suggest that N_2O_5 reactivity on ambient particles should be significantly suppressed (by factors of 2 to 10), with a stronger dependence on RH compared to that expected for aqueous inorganic solution particles. While outside the scope of this paper, including the "nitrate effect", the well-known suppression of N_2O_5 reactivity by particle nitrate aerosol (Bertram and Thornton, 2009; Brown et al., 2009; Mentel et al., 1999; Riedel et al., 2012), only enhances the effect of RH.

4.2   Conclusions

Failing to account for organic components has consistently over-predicted uptake rates of N_2O_5 compared to measured values, even when the nitrate effect is taken into account (Abbatt et al., 2012; Brown et al., 2009; Riedel et al., 2012). Previous studies have shown that organic aerosol has varied effects on N_2O_5 uptake, from near-complete suppression of reactive uptake at small mass fractions (Badger et al., 2006; Cosman and Bertram, 2008; Escorcia et al., 2010; Folkers et al., 2003; Knopf et al., 2007; McNeill et al., 2006; Thornton and Abbatt, 2005), to allowing the same reactivity as inorganic aqueous solutions (Bertram and Thornton, 2009; Griffiths et al., 2009; Thornton et al., 2003). Our results suggest differences in organic composition, such as oxidation state and molecular weight, and the related responses of particle phase, morphology and liquid water content to RH, can explain the different effects of the bulk organic aerosol on N_2O_5 reactivity, and should be factored into parameterizations that account for the presence of organic coatings or variations in particle hygroscopicity.

The key variables for predicting N_2O_5 uptake in the organic coating or pure organic particles are the organic mass fraction in the particles, the diffusivity of N_2O_5 and the liquid water content in the organic layer, the latter two corresponding to the viscosity and hygroscopicity of the organic content (Renbaum-Wolff et al., 2013; Shiraiwa et al., 2011; Virtanen

et al., 2010). We show that for constraining the effects of organic aerosol on N_2O_5 reactivity, the degree of oxidation of the organic aerosol is a useful, but not complete, indicator of these properties, and it is now widely measured during field campaigns and even as part of long-term monitoring activities. We anticipate that our results presented herein together with a growing understanding of organic aerosol properties will help better quantify N_2O_5 reactive uptake onto mixtures of organic and inorganic aerosol in and downwind of polluted regions, thereby further improving predictions made by air quality and climate models. Moreover, N_2O_5 hydrolysis is likely just one of many possible heterogeneous and multiphase processes that may depend similarly on the viscosity, hygroscopicity and mixing state of organic aerosol.

References

Abbatt, J. P. D., Lee, A. K. Y., and Thornton, J. A.: Quantifying trace gas uptake to tropospheric aerosol: recent advances and remaining challenges, Chem. Soc. Rev., 41, 6555–6581, doi:10.1039/c2cs35052a, 2012.

Aiken, A. C. D., Peter, F., Kroll, J. H., Worsnop, D. R., Huffman, J. A., Docherty, K. S., Ulbrich, I. M., Mohr, C., Kimmel, J. R., Sueper, D., Sun, Y., Zhang, Q., Trimborn, A., Northway, M., Ziemann, P. J., Canagaratna, M. R., Onasch, T. B., Alfarra, M. R., Prevot, Andre, S. H., Dommen, J., Duplissy, J., Metzger, A., Baltensperger, U., and Jimenez, J. L.: O / C and OM / OC ratios of primary, secondary, and ambient organic aerosols with high-resolution time-of-flight aerosol mass spectrometry, Environ. Sci. Technol., 42, 4478–4485, 2008.

Alexander, B., Hastings, M. G., Allman, D. J., Dachs, J., Thornton, J. A., and Kunasek, S. A.: Quantifying atmospheric nitrate formation pathways based on a global model of the oxygen isotopic composition ($\Delta^{17}O$) of atmospheric nitrate, Atmos. Chem. Phys., 9, 5043–5056, doi:10.5194/acp-9-5043-2009, 2009.

Anttila, T., Kiendler-Scharr, A., Tillmann, R., and Mentel, T. F.: On the reactive uptake of gaseous compounds by organic-coated aqueous aerosols: Theoretical analysis and application to the heterogeneous hydrolysis of N_2O_5, J. Phys. Chem. A, 110, 10435–10443, 2006.

Badger, C. L., Griffiths, P. T., George, I., Abbatt, J. P. D., and Cox, R. A.: Reactive uptake of N_2O_5 by aerosol particles containing mixtures of humic acid and ammonium sulfate, J. Phys. Chem. A, 110, 6986–6994, 2006.

Bertram, A. K., Martin, S. T., Hanna, S. J., Smith, M. L., Bodsworth, A., Chen, Q., Kuwata, M., Liu, A., You, Y., and Zorn, S. R.: Predicting the relative humidities of liquid-liquid phase separation, efflorescence, and deliquescence of mixed particles of ammonium sulfate, organic material, and water using the organic-to-sulfate mass ratio of the particle and the oxygen-to-carbon elemental ratio of the organic component, Atmos. Chem. Phys., 11, 10995–11006, doi:10.5194/acp-11-10995-2011, 2011.

Bertram, T. H. and Thornton, J. A.: Toward a general parameterization of N_2O_5 reactivity on aqueous particles: the competing effects of particle liquid water, nitrate and chloride, Atmos. Chem. Phys., 9, 8351–8363, doi:10.5194/acp-9-8351-2009, 2009.

Bertram, T. H., Thornton, J. A., Riedel, T. P., Middlebrook, A. M., Bahreini, R., Bates, T. S., Quinn, P. K., and Coffman, D. J.: Direct observations of N_2O_5 reactivity on ambient aerosol particles, Geophys. Res. Lett., 36, L19803, doi:10.1029/2009GL040248, 2009.

Brown, S. S., Dube, W. P., Fuchs, H., Ryerson, T. B., Wollny, A. G., Brock, C. A., Bahreini, R., Middlebrook, A. M., Neuman, J. A., Atlas, E., Roberts, J. M., Osthoff, H. D., Trainer, M., Fehsenfeld, F. C., and Ravishankara, A. R.: Reactive uptake coefficients for N_2O_5 determined from aircraft measurements during the Second Texas Air Quality Study: Comparison to current model parameterizations, J. Geophys. Res.-Atmos., 114, D00F10, doi:10.1029/2008JD011679, 2009.

Canagaratna, M. R.: Improved calibration of O / C and H/C Ratios obtained by aerosol mass spectrometry of organic species, in preparation, 2014.

Chang, W. L., Bhave, P. V., Brown, S. S., Riemer, N., Stutz, J., and Dabdub, D.: Heterogeneous atmospheric chemistry, ambient measurements, and model calculations of N_2O_5: A review, Aerosol Sci. Tech., 45, 665–695, 2011.

Ciobanu, V. G., Marcolli, C., Krieger, U. K., Weers, U., and Peter, T.: Liquid-liquid phase separation in mixed organic/inorganic aerosol particles, J. Phys. Chem. A, 113, 10966–10978, 2009.

Cosman, L. M. and Bertram, A. K.: Reactive uptake of N_2O_5 on aqueous H_2SO_4 solutions coated with 1-component and 2-component monolayers, J. Phys. Chem. A, 112, 4625–4635, 2008.

Denkenberger, K. A., Moffet, R. C., Holecek, J. C., Rebotier, T. P., and Prather, K. A.: Real-time, single-particle measurements of oligomers in aged ambient aerosol particles, Environ. Sci. Technol., 41, 5439–5446, 2007.

Dentener, F. J. and Crutzen, P. J.: Reaction of N_2O_5 on tropospheric aerosols: Impact on the global distributions of NO_x, O_3, and OH, J. Geophys. Res., 98, 7149–7163, 1993.

Duong, H. T., Sorooshian, A., Craven, J. S., Hersey, S. P., Metcalf, A. R., Zhang, X., Weber, R. J., Jonsson, H. H., Flagan, R. C., and Seinfeld, J. H.: Water-soluble organic aerosol in the Los Angeles Basin and outflow regions: Airborne and ground measurements during the 2010 CalNex field campaign, J. Geophys. Res., 116, D00V04, doi:10.1029/2011JD016674, 2011.

Erdakos, G. B. and Pankow, J. F.: Gas/particle partitioning of neutral andionizing compounds to single- and multi-phase aerosol particles. 2. Phase separation in liquid particulate matter containing both polar and low-polarity organic compounds, Atmos. Environ., 38, 1005–1013, 2004.

Escorcia, E. N., Sjostedt, S. J., and Abbatt, J. P. D.: Kinetics of N_2O_5 hydrolysis on secondary organic aerosol and mixed ammonium bisulfate-secondary organic aerosol particles, J. Phys. Chem. A, 114, 13113–13121, 2010.

Finlayson-Pitts, B. J., Ezell, M. J., and Pitts Jr., J. N.: Formation of chemically active chlorine compounds by reactions of atmospheric NaCl particles with gaseous N_2O_5 and $ClONO_2$, Nature, 337, 241–244, 1999.

Folkers, M., Mentel, T. F., and Wahner, A.: Influence of an organic coating on the reactivity of aqueous aerosols probed by the heterogeneous hydrolysis of N_2O_5, Geophys. Res. Lett., 30, 1644, doi:10.1029/2003GL017168, 2003.

Fuchs, N. A. and Sutugin, A. G.: Highly-dispersed aerosols, in: Topics in current aerosol research, edited by: Hidy, G. M. and Brock, J. R., 1–60, Pergamon Press, New York, 1971.

Griffiths, P. T., Badger, C. L., Cox, A., Folkers, M., Henk, H. H., and Mentel, T. F.: Reactive uptake of N_2O_5 by aerosols containing dicarboxylic acids. Effect of particle phase, composition, and nitrate content, J. Phys. Chem. A, 113, 5082–5090, 2009.

Hallquist, M., Stewart, D. J., Stephenson, S. K., and Cox, R. A.: Hydrolysis of N_2O_5 on submicron sulfate aerosols, Phys. Chem. Chem. Phys., 5, 3453–3463, 2003.

Hu, J. H. and Abbatt, J. P. D.: Reaction probabilities for N_2O_5 hydrolysis on sulfuric acid and ammonium sulfate aerosols at room temperature, J. Phys. Chem. A, 101, 871–878, 1997.

Jimenez, J. L., Canagaratna, M. R., Donahue, N. M., Prevot, A. S. H., Zhang, Q., Kroll, J. H., DeCarlo, P. F., Allan, J. D., Coe, H., Ng, N. L., Aiken, A. C., Docherty, K. S., Ulbrich, I. M., Grieshop, A. P., Robinson, A. L., Duplissy, J., Smith, J. D., Wilson, K. R., Lanz, V. A., Hueglin, C., Sun, Y. L., Tian, J., Laaksonen, A., Raatikainen, T., Rautiainen, J., Vaattovaara, P., Ehn, M., Kulmala, M., Tomlinson, J. M., Collins, D. R., Cubison, M. J., Dunlea, E. J., Huffman, J. A., Onasch, T. B., Alfarra, M. R., Williams, P. I., Bower, K., Kondo, Y., Schneider, J., Drewnick, F., Borrmann, S., Weimer, S., Demerjian, K., Salcedo, D., Cottrell, L., Griffin, R., Takami, A., Miyoshi, T., Hatakeyama, S., Shimono, A., Sun, J. Y., Zhang, Y. M., Dzepina, K., Kimmel, J. R., Sueper, D., Jayne, J. T., Herndon, S. C., Trimborn, A. M., Williams, L. R., Wood, E. C., Middlebrook, A. M., Kolb, C. E., Baltensperger, U., and Worsnop, D. R.: Evolution of organic aerosols in the atmosphere, Science, 26, 1525–1529, 2009.

Kalberer, M., Paulsen, D., Sax, M., Steinbacher, M., Dommen, J., Prevot, A. S. H., Fisseha, R., Weingartner, E., Frankevich, V., Zenobi, R., and Baltensperger, U.: Identification of polymers as major components of atmospheric organic aerosols, Science, 303, 1659–1662, 2004.

Kane, S. M., Caloz, F., and Leu, M.-T.: Heterogeneous uptake of gaseous N_2O_5 by $(NH_4)_2SO_4$, NH_4HSO_4, and H_2SO_4 aerosols, J. Phys. Chem. A, 105, 6465–6470, 2001.

Kercher, J. P., Riedel, T. P., and Thornton, J. A.: Chlorine activation by N_2O_5: simultaneous, in situ detection of $ClNO_2$ and N_2O_5 by chemical ionization mass spectrometry, Atmos. Meas. Tech., 2, 193–204, doi:10.5194/amt-2-193-2009, 2009.

Knopf, D. A., Cosman, L. M., Mousavi, P., Mokamati, S., and Bertram, A. K.: A novel flow reactor for studying reactions on liquid surfaces coated by organic monolayers: Methods,

validation, and initial results, J. Phys. Chem. A, 111, 11021–11032, 2007.

Koop, T., Bookhold, J., Shiraiwa, M., and Poschl, U.: Glass transition and phase state of organic compounds: dependency on molecular properties and implications for secondary organic aerosols in the atmosphere, Phys. Chem. Chem. Phys., 13, 19238–19255, 2011.

Kroll, J. H., Donahue, N. M., Jimenez, J. L., Kessler, S. H., Canagaratna, M. R., Wilson, K. R., Altieri, K. E., Mazzoleni, L. R., Wozniak, A. S., Bluhm, H., Mysak, E. R., Smith, J. D., Kolb, C. E., and Worsnop, D. R.: Carbon oxidation state as a metric for describing the chemistry of atmospheric organic aerosol, Nature Chemistry, 3, 133–139, 2011.

Liao, H., and Seinfeld, J. H.: Global impacts of gas-phase chemistry-aerosol interactions on direct radiative forcing by anthropogenic aerosols and ozone, J. Geophys. Res., 110, D18208, doi:10.1029/2005JD005907, 2005.

Lopez-Hilfiker, F. D., Constantin, K., Kercher, J. P., and Thornton, J. A.: Temperature dependent halogen activation by N_2O_5 reactions on halide-doped ice surfaces, Atmos. Chem. Phys., 12, 5237–5247, doi:10.5194/acp-12-5237-2012, 2012.

Marcolli, C. and Krieger, U. K.: Phase changes during hygroscopic cycles of mixed organic/inorganic model systems of tropospheric aerosols, J. Phys. Chem. A, 110, 1881–1893, 2006.

Marcolli, C. and Peter, Th.: Water activity in polyol/water systems: new UNIFAC parameterization, Atmos. Chem. Phys., 5, 1545–1555, doi:10.5194/acp-5-1545-2005, 2005.

Marcolli, C., Luo, B., and Peter, T.: Mixing of the organic aerosol fractions: Liquids as the thermodynamically stable phases, J. Phys. Chem. A, 108, 2216–2224, 2004.

Martin, S. T.: Phase transitions of aqueous atmospheric particles, Chem. Rev., 100, 3403–3453, 2000.

McNeill, V. F., Patterson, J., Wolfe, G. M., and Thornton, J. A.: The effect of varying levels of surfactant on the reactive uptake of N_2O_5 to aqueous aerosol, Atmos. Chem. Phys., 6, 1635–1644, doi:10.5194/acp-6-1635-2006, 2006.

Mentel, T. F., Sohn, M., and Wahner, A.: Nitrate effect in the heterogeneous hydrolysis of dinitrogen pentoxide on aqueous aerosols, Phys. Chem. Chem. Phys., 1, 5451–5457, 1999.

Mozurkewich, M., and Calvert, J. G.: Reaction probability of N_2O_5 on aqueous aerosols, J. Geophys. Res., 93, 15889–15896, 1988.

Murphy, D. M., Cziczo, D. J., Froyd, K. D., Hudson, P. K., Matthew, B. M., Middlebrook, A. M., Peltier, R. E., Sullivan, A., Thomson, D. S., and Weber, R. J.: Single-particle mass spectrometry of tropospheric aerosol particles, J. Geophys. Res.-Atmos., 111, D23S32, doi:10.1029/2006JD007340, 2006.

Ng, N. L., Canagaratna, M. R., Zhang, Q., Jimenez, J. L., Tian, J., Ulbrich, I. M., Kroll, J. H., Docherty, K. S., Chhabra, P. S., Bahreini, R., Murphy, S. M., Seinfeld, J. H., Hildebrandt, L., Donahue, N. M., DeCarlo, P. F., Lanz, V. A., Prévôt, A. S. H., Dinar, E., Rudich, Y., and Worsnop, D. R.: Organic aerosol components observed in Northern Hemispheric datasets from Aerosol Mass Spectrometry, Atmos. Chem. Phys., 10, 4625–4641, doi:10.5194/acp-10-4625-2010, 2010.

Ninni, L., Camargo, M. S., and Meirelles, A. J. A.: Water activity in poly (ethylene glycol) aqueous solutions, Thermochim. Acta, 328, 169–176, 1999.

Ninni, L., Camargo, M. S., and Meirelles, A. J. A.: Water activity in polyol systems, J. Chem. Eng. Data, 45, 654–660, 2000.

Osthoff, H. D., Roberts, J. M., Ravishankara, A. R., Williams, E. J., Lerner, B. M., Sommariva, R., Bates, T. S., Coffman, D., Quinn, P. K., Dibb, J. E., Stark, H., Burkholder, J. B., Talukdar, R. K., Meagher, J., Fehsenfeld, F. C., and Brown, S. S.: High levels of nitryl chloride in the polluted subtropical marine boundary layer, Nat. Geosci., 1, 324–328, 2008.

Poschl, U.: Atmospheric aerosols: Composition, transformation, climate and health effects, Angew. Chem.-Int. Edit., 44, 7520–7540, 2005.

Rahbari-Sisakht, M., Taghizadeh, M., and Eliassi, A.: Densities and viscosities of binary mixtures of poly(ethylene glycol) and poly(propylene glycol) in water and ethanol in the 293.15–338.15 K temperature range, J. Chem. Eng. Data, 48, 1221–1224, 2003.

Reid, J. P., Dennis-Smither, B. J., Kwamena, N.-O. A., Miles, R. E. H., Hanford, K. L., and Homer, C. J.: The morphology of aerosol particles consisting of hydrophobic and hydrophilic phases: Hydrocarbons, alcohols and fatty acids as the hydrophobic component, Phys. Chem. Chem. Phys., 13, 15559–15572, 2011.

Renbaum-Wolff, L., Grayson, J. W., Bateman, A. P., Kuwata, M., Sellier, M., Murray, B. J., Shilling, J. E., Martin, S. T., and Bertram, A. K.: Viscosity of α-pinene secondary organic material and implications for particle growth and reactivity, P. Natl. Acad. Sci. USA, 110, 8014–8019, doi:10/1073/pnas.1219548110, 2013.

Riedel, T. P., Bertram, T. H., Ryder, O. S., Liu, S., Day, D. A., Russell, L. M., Gaston, C. J., Prather, K. A., and Thornton, J. A.: Direct N_2O_5 reactivity measurements at a polluted coastal site, Atmos. Chem. Phys., 12, 2959–2968, doi:10.5194/acp-12-2959-2012, 2012.

Riemer, N., Vogel, H., Vogel, B., Anttila, T., Kiendler-Scharr, A., and Mentel, T. F.: Relative importance of organic coatings for the heterogeneous hydrolysis of N_2O_5 during summer in Europe, J. Geophys. Res., 114, D17307, doi:10.1029/2008JD011369, 2009.

Saukko, E., Lambe, A. T., Massoli, P., Koop, T., Wright, J. P., Croasdale, D. R., Pedernera, D. A., Onasch, T. B., Laaksonen, A., Davidovits, P., Worsnop, D. R., and Virtanen, A.: Humidity-dependent phase state of SOA particles from biogenic and anthropogenic precursors, Atmos. Chem. Phys., 12, 7517–7529, doi:10.5194/acp-12-7517-2012, 2012.

Shindell, D. T., Faluvegi, G., Koch, D. M., Schmidt, G. A., Unger, N., and Bauer, S. E.: Improved attribution of climate forcing to emissions, Science, 326, 716–718, 2009.

Shiraiwa, M., Ammann, M., Koop, T., and Poschl, U.: Gas uptake and chemical aging of semi-solid organic aerosol particles, P. Natl. Acad. Sci., 108, 11003–11008, 2011.

Solomon, S.: Stratospheric ozone depletion: A review of concepts and history, Rev. Geophys., 37, 275–316, 1999.

Song, M., Marcolli, C., Krieger, U. K., Zuend, A., and Peter, T.: Liquid-liquid phase separation and morphology of internally mixed dicarboxylic acids/ammonium sulfate/water particles, Atmos. Chem. Phys., 12, 2691–2712, doi:10.5194/acp-12-2691-2012, 2012.

Surratt, J. D., Murphy, S. M., Kroll, J. H., Ng, N. L., Hildebrandt, L., Sorooshian, A., Szmigielski, R., Vermeylen, R., Maenhaut, W., Claeys, M., Flagan, R. C., and Seinfeld, J. H.: Chemical composition of secondary organic aerosol formed from the photooxidation of isoprene, J. Phys. Chem. A, 110, 9665–9690, 2006.

Tang, I. N. and Munkelwitz, H. R.: Aerosol growth studies – III Ammonium bisulfate aerosols in a moist atmosphere, J. Aerosol Sci., 8, 321–330, 1977.

Tang, I. N. and Munkelwitz, H. R.: Water activities, densities, and refractive indices of aqueous sulfates and sodium nitrate droplets of atmospheric importance, J. Geophys. Res., 99, 18801–18808, 1994.

Thornton, J. A. and Abbatt, J. P. D.: N$_2$O$_5$ reaction on submicron sea salt aerosol: Kinetics, products, and the effect of surface active organics, J. Phys. Chem. A, 109, 10004–10012, 2005.

Thornton, J. A., Braban, C. F., and Abbatt, J. P. D.: N$_2$O$_5$ hydrolysis on sub-micron organic aerosols: the effect of relative humidity, particle phase, and particle size, Phys. Chem. Chem. Phys., 5, 4593–4603, 2003.

Thornton, J. A., Kercher, J. P., Riedel, T. P., Wagner, N. L., Cozic, J., Holloway, J. S., Dube, W. P., Wolfe, G. M., Quinn, P. K., Middlebrook, A. M., Alexander, B., and Brown, S. S.: A large atomic chlorine source inferred from mid-continental reactive nitrogen chemistry, Nature, 464, 271–274, 2010.

Virtanen, A., Joutsensaari, J., Koop, T., Kannosto, J., Yli-Pirila, P., Leskinen, J., Makela, J. M., Holopainen, J. K., Poschl, U., Kulmala, M., Worsnop, D. R., and Laaksonen, A.: An amorphous solid state of biogenic secondary organic aerosol particles, Nature, 467, 824–827, 2010.

Wagner, N. L., Riedel, T. P., Young, C. J., Bahreini, R., Brock, C. A., Dube, W. P., Kim, S., Middlebrook, A. M., Ozturk, F., Roberts, J. M., Russo, R. S., Sive, B. C., Swarthout, R., Thornton, J. A., VandenBoer, T. C., Zhou, Y., and Brown, S. S.: N$_2$O$_5$ uptake coefficients and nocturnal NO$_2$ removal rates determined from ambient wintertime measurements, J. Geophys. Res., 118, 9331–9350, doi:10.1002/jgrd.50653, 2013.

You, Y., Renbaum-Wolff, L., Carreras-Sospedra, M., Hanna, S. J., Hiranuma, N., Kamal, S., Smith, M. L., Zhang, X., Weber, R. J., Shilling, J. E., Dabdub, D., Martin, S. T., and Bertram, A. K.: Images reveal that atmospheric particles can undergo liquid-liquid phase separations, P. Natl. Acad. Sci. USA, 109, 13188–13193, doi:10.1073/pnas.1206414109, 2012.

You, Y., Renbaum-Wolff, L., and Bertram, A. K.: Liquid–liquid phase separation in particles containing organics mixed with ammonium sulfate, ammonium bisulfate, ammonium nitrate or sodium chloride, Atmos. Chem. Phys., 13, 11723–11734, doi:10.5194/acp-13-11723-2013, 2013.

Zhang, Q., Jimenez, J. L., Canagaratna, M. R., Allan, J. D., Coe, H., Ulbrich, I. M., Alfarra, M. R., Takami, A., Middlebrook, A. M., Sun, Y. L., Dzepina, K., Dunlea, E., Docherty, K. S., DeCarlo, P. F., Salcedo, D., Onasch, T. B., Jayne, J. T., Miyoshi, T., Shimono, A., Hatakeyama, S., Takegawa, N., Kondo, Y., Schneider, J., Drewnick, F., Borrmann, S., Weimer, S., Demerjian, K., Williams, P., Bower, K., Bahreini, R., Cottrell, L., Griffin, R. J., Rautiainen, J., Sun, J. Y., Zhang, Y. M., and Worsnop, D. R.: Ubiquity and dominance of oxygenated species in organic aerosols in anthropogenically-influenced Northern Hemisphere midlatitudes, Geophys. Res. Lett., 34, L13801, doi:10.1029/2007GL029979, 2007.

Zobrist, B., Marcolli, C., Pedernera, D. A., and Koop, T.: Do atmospheric aerosols form glasses?, Atmos. Chem. Phys., 8, 5221–5244, doi:10.5194/acp-8-5221-2008, 2008.